

Resistive Wall Mode Stabilization and Plasma Rotation Damping Considerations for Maintaining High Beta Plasma Discharges in NSTX

S.A. Sabbagh 1), J.W. Berkery 1), J.M. Bialek 1), R.E. Bell 2), S.P. Gerhardt 2), O.N. Katsuro-Hopkins 1), J.E. Menard 2), H. Reimerdes 1), R. Betti 2,3), L. Delgado-Aparicio 2), D.A. Gates 2), B. Hu 3), B.P. LeBlanc 2), J. Manickam 2), D. Mastrovito 2), J.-K. Park 2), Y.-S. Park 1), K. Tritz 4)

1) Department of Applied Physics and Applied Mathematics, Columbia University, New York, NY, USA

2) Princeton Plasma Physics Laboratory, Princeton University, Princeton, NJ, USA

3) Laboratory for Laser Energetics, University of Rochester, Rochester, NY, USA

4) Johns Hopkins University, Baltimore, MD, USA

e-mail contact of main author: sabbagh@pppl.gov

Abstract. Maintaining steady fusion power output at high plasma beta is an important goal for future burning plasmas such as in ITER advanced scenario operation and a fusion nuclear science facility. Research on the National Spherical Torus Experiment (NSTX) is investigating stability and control physics to maintain steady high plasma normalized beta with minimal fluctuation. Resistive wall mode (RWM) instability is observed at relatively high rotation levels. Analysis including kinetic effects using the MISC code shows a region of reduced stability for marginally stable experimental plasmas caused by the rotation profile falling between stabilizing ion precession drift and bounce/transit resonances. Energetic particle (EP) effects are stabilizing but weaker than in tokamaks due to a reduced EP population in the outer plasma. Calculations for ITER show that alpha particles are required to stabilize the RWM at anticipated rotation levels for normalized beta of 3. Combined RWM and new beta feedback control capability were used to generate high pulse-averaged normalized beta with low fluctuation. Non-resonant braking by applied 3-D fields was used to alter plasma rotation compatibly with beta feedback. A newly implemented RWM state space controller produced long pulse, high normalized beta plasmas at low internal inductance. Neoclassical toroidal viscosity (NTV) torque by applied 3-D fields could be used to actuate rotation control and avoid rotation profiles unfavorable for RWM stability. As the ExB frequency is reduced, the NTV torque is expected to increase as collisionality decreases, and maximize when it falls below the ∇B drift frequency (superbanana plateau regime). Increased non-resonant braking was observed at constant applied field and normalized beta in experiments when rotation and ExB frequency were reduced to low values. The RWM multi-mode spectrum is computed in high beta plasmas using the multi-mode VALEN code. The computed RWM growth rate for instabilities and natural mode rotation for stabilized modes agrees with experiment. The computed multi-mode RWM spectrum shows significant amplitude in low-order ideal eigenfunctions other than the least-stable eigenfunction of single-mode analysis.

1. Introduction

Maintaining steady fusion power output at high plasma beta is an important goal for future burning plasmas such as in ITER advanced scenario operation and spherical torus (ST) applications such as a fusion nuclear science facility/component test facility (FNSF/CTF) [1] and an ST pilot plant [2]. Plasmas in the National Spherical Torus Experiment (NSTX) have reached plasma normalized beta, $\beta_N \equiv 10^8 \langle \beta_t \rangle a B_0 / I_p = 7.4$ transiently ($\beta_t \equiv 2\mu_0 \langle p \rangle / B_0^2$). Present research investigates the stability physics and control to maintain steady high β_N greater than 5 with minimal fluctuation. As ITER and FNSF span a wide range of plasma toroidal rotation angular frequency, ω_ϕ , from low to high, stability physics needs to be understood in these regimes. Variation of ω_ϕ is also critically important as resistive wall modes (RWM) are observed to become unstable at ω_ϕ levels far greater than previously reported in tokamaks [3] and that stability depends on ω_ϕ profile resonances [4,5]. This research is part of a broad ranging effort on NSTX to maintain high beta plasmas in steady-state via plasma shaping, lithium wall coating, and error field reduction [6-8].

NSTX can operate at high β_N above the $n = 1$ no-wall ideal stability limit with resistive wall modes stabilized by passive means [9]. Nevertheless, RWMs are observed to destabilize at high ω_ϕ in NSTX, and active RWM control is used to suppress these instabilities [5,10]. The observed mode has a strong $n = 1$ component with growth rate of the order of the inverse resistive wall eddy current decay time, and rotates in the direction of neutral beam injection if it unlocks during growth (Fig. 1(a)). Such an instability at high and relatively peaked ω_ϕ is shown in Fig. 1(a), with the unstable ω_ϕ profile shown in Fig. 1(b). In contrast, plasmas with broader ω_ϕ tend to be RWM stable, and can remain stable as ω_ϕ is reduced by non-resonant $n = 3$ magnetic braking [11]. The proximity of these stable plasmas to marginal stability as ω_ϕ is reduced can be evaluated by active MHD spectroscopy [12]. The result of such a discharge evolution is shown in Fig. 1(b-e). Plasma rotation was slowed by $n = 3$ magnetic braking (Fig. 1(b)). At $t = 0.6$ s, active $n = 1$ RWM feedback control is turned off, and an $n = 1$, 40 Hz co-NBI propagating tracer field is applied (Fig. 1(c)) to evaluate the resonant field amplification (RFA) caused by the high β_N plasma. During this time β_N is relatively constant (Fig. 1(d)), yet the RFA amplitude increases and decreases as ω_ϕ is reduced (Fig. 1(e)) indicating that the plasma first approaches, then departs from RWM marginal stability. Note that the RWM unstable plasma shown occurs at *lower* $\beta_N = 4.7$, while the stable plasma exceeds $\beta_N = 6.5$.

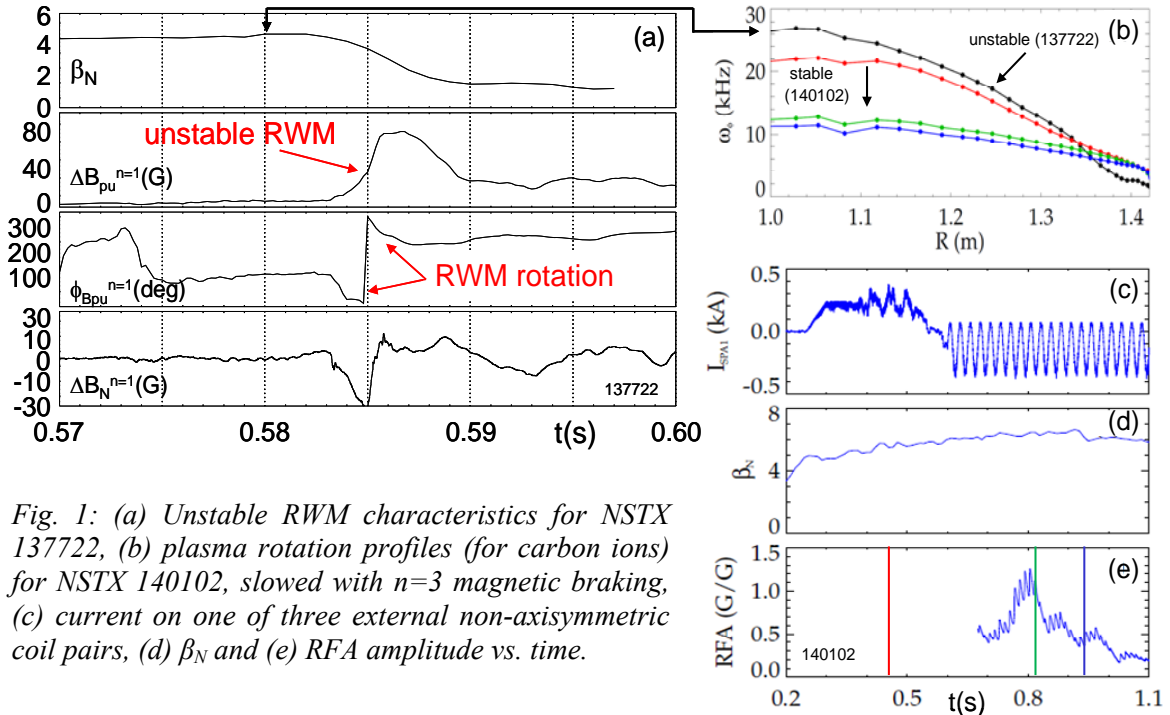


Fig. 1: (a) Unstable RWM characteristics for NSTX 137722, (b) plasma rotation profiles (for carbon ions) for NSTX 140102, slowed with $n=3$ magnetic braking, (c) current on one of three external non-axisymmetric coil pairs, (d) β_N and (e) RFA amplitude vs. time.

In Sec. 2, these characteristics of RWM stability are compared with kinetic stability theory. Section 3 discusses improved active RWM feedback with both poloidal and radial sensors, combined with neutral beam feedback to minimize β_N fluctuation, and results from a newly-implemented RWM state space controller. The physics of non-resonant ω_ϕ damping by 3-D fields [13], a candidate for ω_ϕ control actuation in devices with strong momentum input, is investigated versus the ExB frequency, ω_E , in Sec. 4. In Sec. 5, the multi-mode RWM spectrum at high β_N , that in theory can significantly affect control, is examined.

2. Resistive Wall Mode Stability Dependence on Rotation and Energetic Particles

Understanding and maximizing passive RWM stabilization by ω_ϕ and energetic particles (EPs) will reduce demands on active control systems, potentially allowing control coils to be moved farther away from regions of high neutron flux in future devices. As shown in Sec. 1,

the RWM can become unstable in NSTX plasmas with relatively high plasma rotation, compared to the predictions of classic models, which predict a low “critical” rotation sufficient to stabilize the mode [14] and compared to experiments in DIII-D [15]. This indicates that further physics understanding is required to confidently extrapolate RWM stability to future devices. Analysis of the RWM stability criterion for NSTX plasmas adding kinetic dissipation effects [16] incorporated in the MISK code [17] explains how NSTX plasmas can become unstable at relatively high levels of ω_ϕ . The RWM growth rate normalized by the wall time, $\gamma\tau_w$, is calculated with the RWM dispersion relation including kinetic effects: $(\gamma - i\omega_r)\tau_w = -(\delta W_\infty + \delta W_K)/(\delta W_b + \delta W_K)$ where ω_r is the mode rotation frequency, and δW_b and δW_∞ are the with and without-wall potential energies, calculated with the PEST code. The MISK code calculates the change in potential energy due to kinetic effects, δW_K , for trapped and circulating thermal ions, trapped electrons, trapped energetic particles, and Alfvén layers at the rational surfaces [18]. The calculation involves integration over flux surfaces, pitch angle, and energy of a term involving resonances between ω_E and the precession drift frequency, ω_D , and bounce, ω_b , or transit frequencies, with plasma collisionality, ν_{eff} , also included:

$$\delta W_K \propto \int \left[\frac{\omega_{*N} + \left(\hat{\epsilon} - \frac{3}{2}\right)\omega_{*T} + \omega_E - \omega_r - i\gamma}{\langle\omega_D\rangle + l\omega_b - i\nu_{eff} + \omega_E - \omega_r - i\gamma} \right] \hat{\epsilon}^{\frac{5}{2}} e^{-\hat{\epsilon}} d\hat{\epsilon}. \quad (1)$$

We first consider the effect of ω_ϕ and ν_{eff} on RWM stability using the plasma thermal pressure. Plasma rotation appears in Eq. (1) through $\omega_E = \omega_\phi - \omega_{*N} - \omega_{*T}$, where ω_{*N} and ω_{*T} are the density and temperature gradient components of the diamagnetic frequency. An NSTX plasma with decreasing ω_ϕ that became RWM unstable was analyzed by MISK (Fig. 2). The

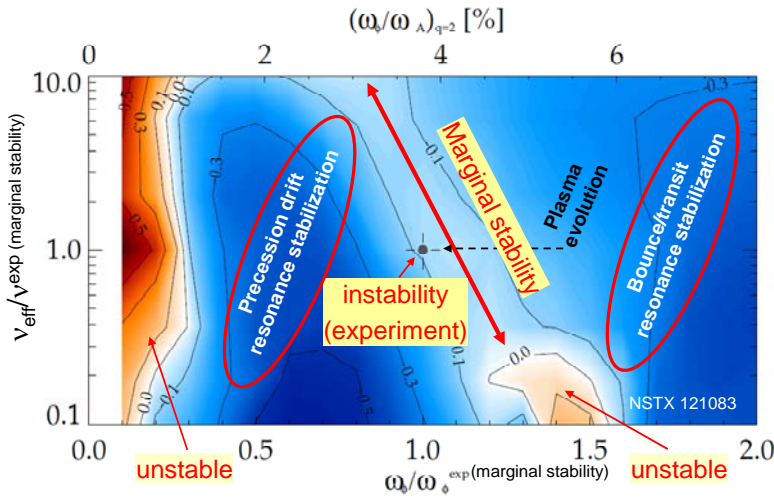


Fig. 2: RWM growth rate contours normalized to wall current decay time, $\gamma\tau_w$, for marginally stable NSTX plasma (MISK).

ω_ϕ is decreased, and is similar to the analysis of an analogous DIII-D experiment [19]. The physical cause for the stability reduction in Fig. 2 is ω_ϕ falling between the stabilizing ion precession drift and bounce/transit resonances (Eq. (1)) [4]. For reference, this occurs at $\omega_\phi/\omega_{Alfven} \sim 3.8\%$ near the $q = 2$ surface, however that there is no particular importance of the $q = 2$ surface in this theory. The figure also illustrates the dependence of the reduced stability on ν_{eff} , an important consideration for extrapolation to future devices. Decreasing ν_{eff} shows an increase in the higher ω_ϕ level at which the RWM becomes unstable.

The next consideration in the MISK analysis is the effect of energetic particles (EPs) on δW_k . Details of the present MISK model for energetic particles are given in reference [18]. In

the experimental marginally stable ω_ϕ profile, ω_ϕ^{exp} , is indicated in Fig. 2 by the abscissa value of unity. As the discharge evolved from higher to lower ω_ϕ , MISK shows the plasma becoming less stable as it approached the marginal point. As ω_ϕ is reduced further, the plasma gains stability. This computed stability evolution is consistent with the observation of first increasing, then decreasing RFA amplitude in NSTX as

both MISK analysis and dedicated NSTX experiments varying the EP content at fixed q , the RWM becomes more stable as energetic ion pressure is increased, but variation of ω_ϕ has a larger effect on RWM growth rate than do the energetic particles. This result can explain why the RWM can become unstable in NSTX as ω_ϕ is varied at relatively high levels, while a similar result is not found in DIII-D where the effect of the EPs on RWM stability is larger. RWM stability analysis with MISK shows weaker EP stabilization in NSTX due to the reduced EP population in the outer portion of the plasma compared to DIII-D. This is shown in Fig. 3, that compares δW_K due to energetic particles in NSTX and DIII-D to the component of δW_K due to trapped ions. NSTX has significantly less EP stabilization. The rotational

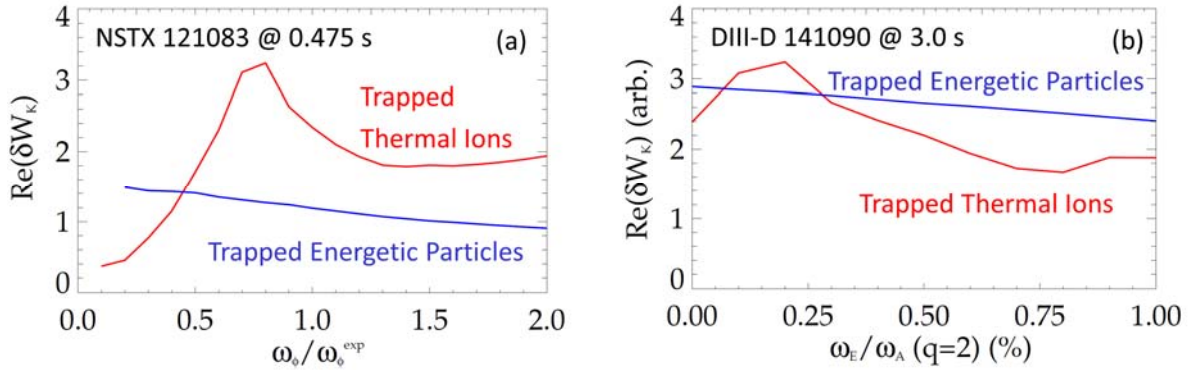


Fig. 3: MISK calculated real δW_K for trapped thermal ions and trapped energetic particles vs. scaled experimental plasma rotation for NSTX and DIII-D plasmas. The plots are scaled so that the peaks of trapped thermal ion $\text{Re}(\delta W_K)$ are the same, to show the relative difference in the EP contribution.

resonances of thermal particles cause the reduction from peak δW_K in Fig. 3. Energetic particles, however, have precession and bounce frequencies that are much larger than the plasma rotation frequency, so they do not resonate. They add a stabilizing force that does not fundamentally change the dependence of stability on ω_ϕ [11]. Fig. 4 illustrates the effect of EPs and rotation on RWM stability using thermal and energetic ion δW_K dependencies on ω_ϕ similar to those in Fig. 3. Kinetic theory, including rotational resonances and energetic particle effects, is consistent with experimental observation and comparison for both NSTX and DIII-D and therefore has the potential to unify the physical explanation of RWM stability across devices. These observations include the result of RWM instability at relatively high

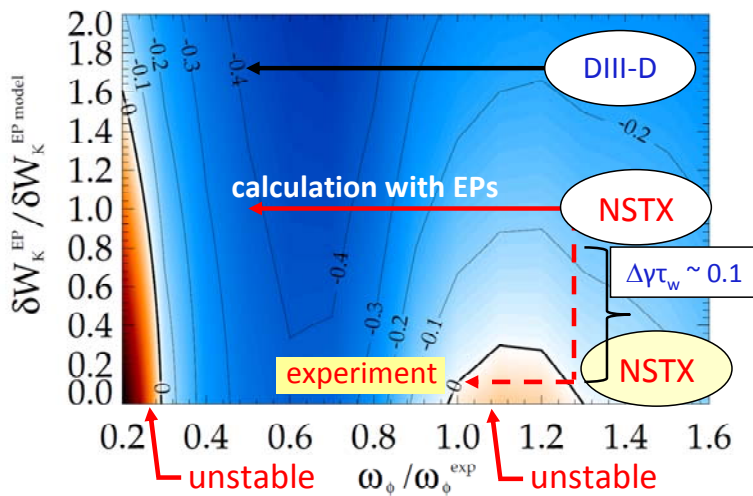


Fig. 4: Stability contours of $\gamma\tau_w$ in an illustrative example, using the δW_K vs. ω_ϕ dependence from Fig. 3(a), showing the effect of EPs and ω_ϕ . Experimental results are consistent with DIII-D and NSTX plasmas being in the regions shown.

ω_ϕ in NSTX, but not in DIII-D, and the decreased plasma rotation necessary for stability with increasing EP content [12]. In the case of DIII-D, MISK analysis shows that energetic particles can indeed stabilize the RWM over the usual operational range of rotation [19], and experimental observation shows that fishbone like modes that reduce EP content can trigger RWM instability [20] (also seen in JT-60U [21]). The present theory is still not completely quantitative, as the stabilizing EP effect appears

too large in NSTX. In Fig. 4, the calculation with EPs bring NSTX above the RWM unstable region at high ω_ϕ , while in experiment, the plasma becomes unstable. However, the difference in $\gamma\tau_w \sim 0.15$ between stability/instability is small – close to the calculation error. We continue to develop the MISK physics model to determine the physical cause for this difference, including a more accurate anisotropic energetic particle distribution.

Similar MISK analysis was applied to ITER advanced scenario IV plasmas to determine the relative importance of ω_ϕ and energetic particles in RWM stabilization. The expected level of rotation in ITER is insufficient for mode stability. At $\beta_N = 3$ (with the ideal no-wall stability limit = 2.5), the alpha particle population expected in ITER ($\beta_\alpha/\beta_{tot} \sim 19\%$) is only just sufficient to bring the RWM to marginal stability.

3. Resistive Wall Mode Active Control Improvements to Maintain High $\langle\beta_N\rangle_{\text{pulse}}$

Combined $n = 1$ resistive wall mode control and newly-implemented β_N feedback control [22] were used to generate high pulse-averaged β_N with low levels of fluctuation at various levels of plasma rotation. A key motivation in performing this experiment was to understand the interaction of the two control systems as plasma rotation was varied by applying different

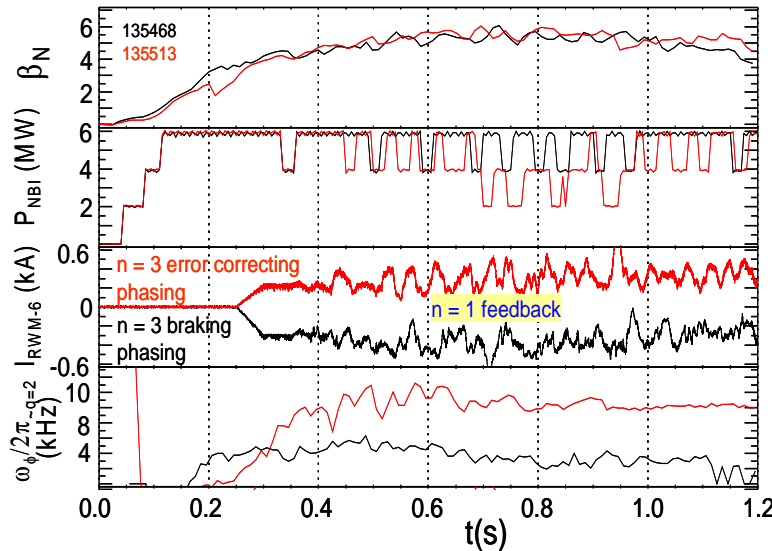


Fig. 5: Maintenance of β_N with low fluctuation at various ω_ϕ by use of $n = 1$ and β_N feedback, and $n = 3$ NTV braking.

with β_N feedback. The discharge with higher ω_ϕ has higher plasma energy confinement time, and therefore requires lower NBI power to maintain constant β_N . Steps in NBI power are dictated by feedback control to maintain constant β_N , but not to maintain plasma rotation. Despite this, ω_ϕ reaches an approximate steady state near $q = 2$ in these plasmas (Fig. 5). The RWM sensor signals used for $n = 1$ mode feedback control were recently compensated for eddy currents due to the AC control fields and OHxTF pickup particularly important for the RWM radial field sensors. Favorable feedback phase and gain settings were found in controlled experiments for both the poloidal and radial field RWM sensor arrays (48 coils total). With the stated compensations, the optimal RWM B_R sensor feedback phase for negative feedback is close to 180 degrees as expected by theory, and these sensors are now routinely used in the RWM feedback control of most experiments. Dedicated experiments have shown high success in stabilizing low l_i plasmas. Plasmas with near record ratios in NSTX of β_N/l_i between 12 – 13 have been produced in controlled sequences of several

levels of $n = 3$ non-resonant magnetic field. A comparison of two successful long-pulse discharges using both $n = 1$ RWM feedback and β_N control at significantly different levels of plasma rotation is shown in Fig. 5. Non-resonant magnetic braking by applied 3D fields due to neoclassical toroidal viscosity (NTV) [23] was used to vary ω_ϕ [11]. Producing steady ω_ϕ using this drag mechanism (shown in NSTX to increase with ion temperature, consistent with a $T_i^{5/2}$ dependence expected by theory [5]) is shown to be compatible

repeated long pulse shots with high success, compared to equivalent plasmas produced last year that suffered RWM-induced disruptions in nearly 50% of the cases run.

An advanced RWM state space controller was newly-implemented in 2010, using a reduced order model of the 3D conducting structure of NSTX and $n = 1$ ideal plasma instability eigenfunctions computed by the DCON code with varied phase to allow the controller to track mode rotation. Of particular interest is the theoretical expectation of the controller to stabilize high beta plasmas with conducting structure (e.g. vessel/plates in NSTX [24], blanket in ITER [25]) between the plasma and the control coils. This ability is especially important for burning plasma devices, where control coils will require greater shielding. NSTX is a superior device to test such a controller for ITER and CTF, as the RWM control coils on the device are external to the machine vacuum vessel, but still closely coupled to both the plasma and device conducting structure. The theoretical performance of the controller for plasmas with an insignificant level of passive stabilization is shown in Fig. 6(a). Using the plasma eigenfunction and wall response for an equilibrium near the no-wall limit (labeled input 2, Fig. 6(a)), the plasma can be controlled up to $\beta_N \sim 6.2$. Using input for an equilibrium near the with-wall limit (input 1, Fig. 6(a)), the plasma can be controlled up to $\beta_N \sim 6.9$, close to the with-wall β_N limit of 7.1. For comparison, the maximum stabilized β_N for a

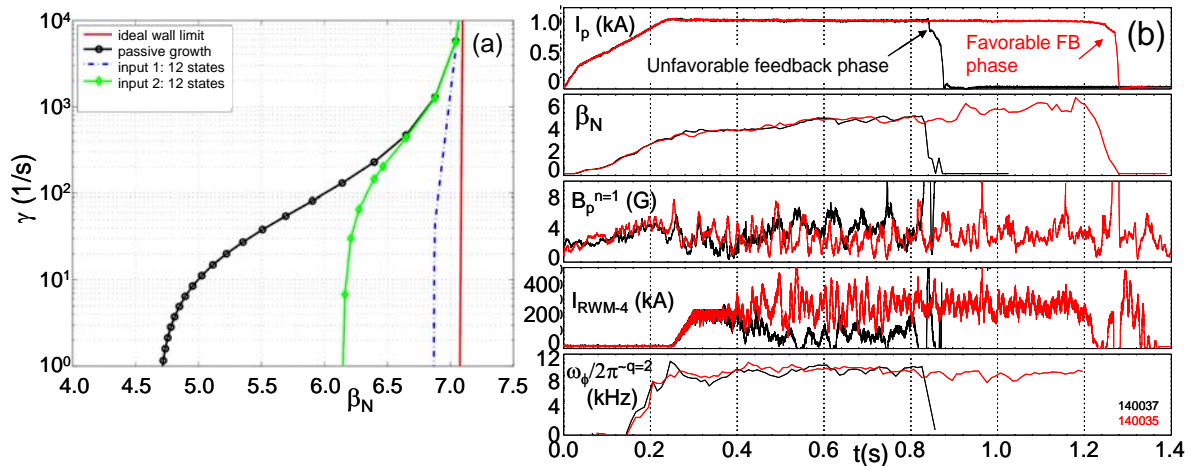


Fig. 6: (a) Theoretical performance of NSTX RWM state space controller (mode growth rate vs. β_N), (b) Feedback phase variation for RWM state space controller. Favorable feedback phase allowed long pulse plasmas with steady plasma rotation and very high stability parameters $\beta_N > 6.4$, $\beta_N/l_i > 13$.

proportional gain controller assuming no significant passive stabilization is 5.6 [5]. In the initial experiments, resonant field amplification due to applied $n = 1$ DC fields sufficiently large to cause plasma disruption, was adequately reduced to allow stable plasma operation. Variation of the feedback phase showed both favorable and unfavorable settings (Fig. 6(b)) shows two feedback phase settings differing by 180 degrees). The best settings produced a stable, long pulse (limited by magnet heating constraints), low l_i plasma with $\beta_N > 6.4$, and $\beta_N/l_i > 13$, the highest value for a stable plasma at high plasma current ($I_p = 1\text{MA}$).

4. Alteration of Plasma Rotation by Non-resonant Fields and Dependence on ω_E

Non-resonant magnetic braking by applied 3-D fields due to neoclassical toroidal viscosity (NTV) [23] could be used to actuate plasma rotation control in devices heated by unidirectional NBI (e.g. in CTF) to avoid ω_ϕ levels and profiles unfavorable for RWM stability discussed above. Understanding the behavior of NTV braking vs. ω_ϕ is important for its

eventual use in a rotation control system. The NTV braking torque, τ_{NTV} , that scales as $|\delta\mathbf{B}|^2\omega_\phi$ where $|\delta\mathbf{B}|$ is the applied 3-D field magnitude, has produced predictable, controlled changes to ω_ϕ in NSTX, usually by applied fields dominated by the $n = 3$ component. Prior experiments on NSTX have also demonstrated non-resonant braking by an $n = 2$ field configuration, and that the NTV braking torque increases with ion temperature, consistent

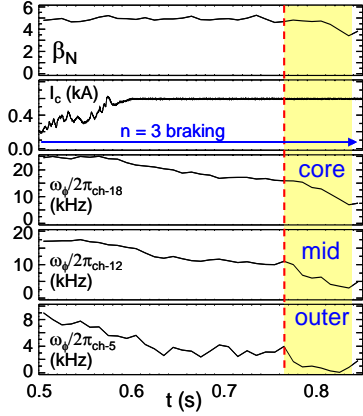
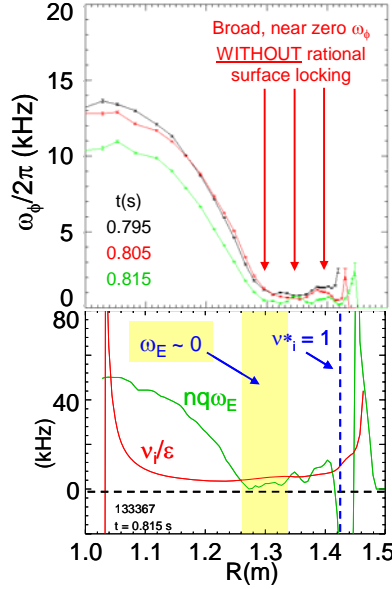


Fig. 7: Increased non-resonant magnetic braking at fixed applied field and β_N at low ω_E .



with the scaling $\tau_{NTV} \sim \delta B^2 \varepsilon^{1.5} p_i / v_i \sim T_i^{5/2}$ expected by theory in the “ $1/\nu$ ” regime [5]. Recent experiments have varied the ratio of ion collisionality to the $E \times B$ frequency, ω_E , a key parameter that determines the scaling of NTV with v_i in the collisionless regime ($v_i^* < 1$). As $|\omega_E|$ is reduced, τ_{NTV}/ω_ϕ is expected to scale as $1/v_i$ when $(v_i/\varepsilon)/(nq|\omega_E|) > 1$ and maximize when it falls below the ∇B drift frequency and enters the superbanana plateau regime [26]. This regime is also most

relevant and important for application to ITER. Lithium wall preparation was used to suppress resonant braking and mode locking due to NTMs, allowing the investigation of non-resonant NTV braking down to low values of ω_ϕ and $|\omega_E|$. Increased braking strength was observed at constant $|\delta\mathbf{B}|$ and β_N in experiments when ω_ϕ (and $|\omega_E|$) were sufficiently decreased, as expected by NTV theory (Fig. 7).

5. Multi-mode RWM Computed Spectrum at High Beta

In high β_N plasmas, the influence of multiple RWM eigenfunctions on $n = 1$ active feedback, including the stable mode spectrum, is a potential cause of β_N fluctuation and loss of control. The newly-developed multi-mode VALEN code has been applied to NSTX experiments to determine the multi-mode RWM spectrum and characteristics. The multi-mode response is theoretically computed to be significant in these plasmas when $\beta_N > 5.2$, based on the criterion of Boozer [27]. The perturbed normal field due to induced wall currents shows the influence of the passive conducting plates (Fig. 8(a)). The computed RWM growth time vs. β_N is in the range observed when such modes are destabilized (Fig. 8(b)). The computed spectrum of eigenfunctions comprising the total perturbed field (Fig. 8(c)) is shown for an unstable mode, and one stabilized by plasma rotation. The RWM multi-mode spectra consist of ideal eigenfunctions computed by the DCON code. These multi-mode components are ordered from lower to higher number, with the lowest number being least stable when each eigenfunction is considered separately in ideal MHD theory. Both spectra show significant amplitude in eigenfunctions up to 10, with the *second* mode component having the maximum amplitude. Poloidal cross-sections of the mode components are also shown. Component 1 is ballooning, while component 2, which has dominant amplitude, has maximum perturbation near the lower divertor. There is a significant change in the multi-mode spectrum for the stabilized plasma. In this case, the ballooning component of the perturbation is significantly reduced compared to the component with maximum perturbation in the lower divertor region. The rotationally stabilized multi-mode RWM has a computed rotation frequency of 41 Hz,

close to the ~ 30 Hz frequency measured in experiments with both magnetic and kinetic diagnostics (soft X-ray). Similar calculations for ITER scenario IV plasmas with elevated q_0 , $\beta_N = 4$, and a modeled blanket conducting structure show multi-mode RWM spectra with up to 6 components of significant amplitude both for unstable $n = 1$ and $n = 2$ modes.

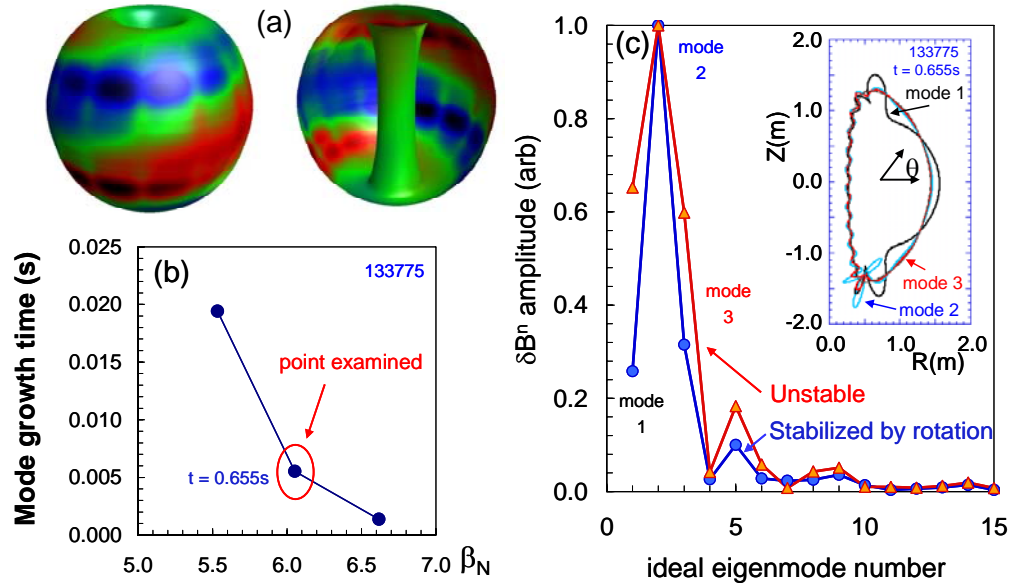


Fig. 8: Multi-mode RWM analysis of high β_N plasmas (a) δB_{normal} from wall currents, (b) growth time vs. β_N for unstable modes, (c) ideal eigenmode spectrum of multi-mode RWM perturbation showing the spectrum of an unstable mode, and one stabilized by plasma rotation.

This research was supported by the U.S. Department of Energy under contracts DE-FG02-99ER54524 and DE-AC02-09CH11466.

- [1] PENG, Y.-K. M., BURGESS, T.W., CARROLL, A.J., *et al.*, Fus. Sci. and Tech. **56** (2009) 957.
- [2] MENARD, J.E., BROMBERG, L., BROWN, T., *et al.*, paper FTP/2-2 this conference.
- [3] GAROFALO, A.M., JACKSON, G., LA HAYE, R., *et al.*, Nucl. Fusion **47** (2007) 1121.
- [4] BERKERY, J.W., SABBAGH, S.A., BETTI, R., *et al.*, Phys. Rev. Lett. **104** (2010) 035003.
- [5] SABBAGH, S.A., BERKERY, J.W., BELL, R.E., *et al.*, Nucl. Fusion **50** (2010) 025020.
- [6] GATES, D.A., AHN, J., ALLAIN, J., *et al.*, Nucl. Fusion **49** (2009) 104016.
- [7] KUGEL, H.W., BELL, M.G., BELL, R.E., *et al.*, J. Nucl. Mater. **363** (2007) 791.
- [8] MENARD, J.E., BELL, R.E., GATES, D.A., *et al.*, Nucl. Fusion **50** (2010) 045008.
- [9] SABBAGH, S.A., SONTAG, A.C., BIALEK, J.M., *et al.*, Nucl. Fusion **46** (2006) 635.
- [10] SABBAGH, S.A., BELL, R.E., MENARD, J.E., *et al.*, Phys. Rev. Lett. **97** (2006) 045004.
- [11] ZHU, W., SABBAGH, S.A., BELL, R.E., *et al.*, Phys. Rev. Lett. **96** (2006) 225002.
- [12] REIMERDES, H., CHU, M.S., GAROFALO, A.M., *et al.*, Phys. Rev. Lett. **93** (2004) 135002.
- [13] SHAINING, K.C., SABBAGH, S.A., and CHU, M.S., Plasma Phys. Control. Fusion **51** (2009) 035004.
- [14] FITZPATRICK, R. and AYDEMIR, A., Nucl. Fusion **36** (1996) 11.
- [15] REIMERDES, H., GAROFALO, A.M., JACKSON, *et al.*, Phys. Rev. Lett. **98** (2007) 055001.
- [16] HU, B. and BETTI, R., Phys. Rev. Lett., **93** (2004) 105002.
- [17] HU, B., BETTI, R., and MANICKAM, J., Phys. Plasmas, **12** (2005) 057301.
- [18] BERKERY, J.W., SABBAGH, S.A., REIMERDES, H., *et al.* Phys. Plasmas **17** (2010) 082504.
- [19] REIMERDES, H., BERKERY, J.W., LANCTOT, M.J., *et al.*, paper EXS/5-4 this conference.
- [20] OKABAYASHI, M., BOGATU, I.N., CHANCE, M.S., *et al.*, Nucl. Fusion **49** (2009) 125003.
- [21] MATSUNAGA, G., AIBA, N., SHINOHARA, K., *et al.*, Phys. Rev. Lett. **103** (2009) 045001.
- [22] GERHARDT, S.P., *et al.*, "Implementation of β_N control in NSTX", submitted to Fus. Sci. and Tech.
- [23] SHAINING, K.C., HIRSHMAN, S.P., and CALLEN, J.D., Phys. Fluids **29** (1986) 521.
- [24] KATSURO-HOPKINS, O.N., SABBAGH, S.A., BIALEK, J.M., *et al.*, "Analysis of resistive wall mode LQG control in NSTX with mode rotation", Proc. 48th IEEE CDC Conf., Shanghai (2009), paper WeA09.5.
- [25] KATSURO-HOPKINS, O.N., BIALEK, J., MAURER, *et al.*, Nucl. Fusion **47** (2007) 1157.
- [26] SHAINING, K.C., SABBAGH, S.A., and CHU, M.S., Plasma Phys. Control. Fusion **51** (2009) 035009.
- [27] BOOZER, A.H., Phys. Plasmas **10** (2003) 1458.